



Removal of fluoride from photovoltaic wastewater by electrocoagulation and products characteristics

N. Drouiche^{a,b*}, H. Lounici^b, M. Drouiche^b, N. Mameri^b, N. Ghaffour^c

^a*Silicon Technology Development Unit (UDTS), 2, Bd Frantz Fanon BP399, Algiers, 16000, Algeria
Tel./Fax +213 21433511; email: najibdrouiche@yahoo.fr*

^b*Laboratory of Environmental Biotechnologies, Ecole nationale Polytechnique d'Alger, 10, Av. Hassene Badi El-Harrach, Algiers, Algeria*

^c*Middle East Desalination Research Center, P.O. Box21, P.C.133, Muscat, Sultanate of Oman*

Received 13 July 2008; accepted ion revised form 9 June 2009

ABSTRACT

Efficient treatment of fluoride-containing wastewater efficiently has been important for environmental engineers in Algeria. An appropriate concentration of fluoride in drinking water is required to prevent dental cavities, but long-term ingestion of water that contains more than a suitable level of fluoride causes bone disease and mottling of the teeth. The CMP wastewater from a UDTS. was characterized by high suspended solids (SS) content, chlorates, hydroxylamine, high turbidity (NTU), chemical oxygen demand (COD) concentration up to 7.00 mg l⁻¹ and fluoride concentration up to 1000 mg l⁻¹. Currently, the cheapest way to remove fluoride from semiconductor wastewater is to produce calcium fluoride (CaF₂) by adding lime or another calcium salt. The aim of this paper is to propose an efficient and low cost treatment of chemical mechanical polishing wastewater process based on electrocoagulation with iron bipolar electrodes. The performance of a pilot scale electrochemical reactor equipped with iron bipolar electrodes and an anode active area surface of about 170 cm² was studied. In addition, sludge settling after electrocoagulation was characterized.

Keywords: Fluoride removal; Physicochemical interaction; Sludge structure; Iron bipolar electrode

1. Introduction

Fluoride is recognized as an essential constituent in the human diet. Low fluoride concentration (< 1 mg/L) could prevent dental problem, but higher fluoride concentration (> 1.5mg/L) will cause dental and skeletal fluorosis [1]. Many countries, such as China, Egypt, India, Taiwan, Senegal, etc., have areas where fluorosis is endemic [2]. Fluoride pollution in environment occurs through two different channels: natural sources and anthropogenic sources. Fluoride is frequently encountered in minerals and in geochemical deposits. Because of the erosion and

weathering of fluoride-bearing minerals, it becomes a surface species. The discharge of industrial wastewater, such as semiconductor industries, aluminum industries, and glass manufacturing industries, also contributes fluoride in water pollution, especially in groundwater.

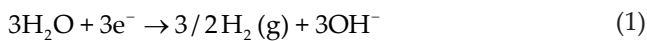
Many methods have been developed to remove excessive fluoride from drinking water. These methods can be categorized into four categories: adsorption [3,4], chemical precipitation [5,6], membrane separation [7,8], and electrocoagulation [9–11]. The electrocoagulation also has successfully been used for the treatment of wastewaters including electroplating wastewater [12], laundry wastewater [13], latex particles [14] and textile wastewaters [15–18]. Meanwhile, EC process has been

* Corresponding author.

widely used to decolorize various structurally different dye containing solutions such as disperse, reactive and acidic dyes [19–22]. Electrocoagulation is a process consisting in creating metallic hydroxide flocks within the wastewater by electro dissolution of soluble anodes, usually made of iron or aluminum [23]. The difference between electrocoagulation and chemical coagulation is mainly in the way aluminum ions are delivered [24]. In electrocoagulation, coagulation and precipitation are not conducted by delivering chemicals – called coagulants – to the system but via electrodes in the reactor [25].

Suitable electrode choice is very important in electrocoagulation. Most common electrode materials are iron and aluminum. Both of these are cheap, easily found and effective materials [26]. When iron is used as electrode materials, the reactions are as follows:

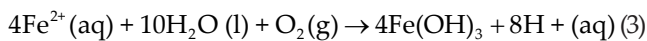
At the cathode:



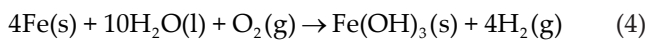
At the anode:



and with dissolved oxygen in solution:



overall reaction:



As can be seen in the above reactions, electrocoagulation is a combination of oxidation, flocculation and flotation. Electrocoagulation occurs in three steps: in the first step, coagulant is formed because of oxidation of anode; in the second step, pollutants are destabilized; and in the last step, destabilized matters are united [27].

2. Experimental

Photovoltaic effluents contain 200–2000 mg/l F^- . The literature [28] reports that by pH adjustment (hydroxide

precipitation) in the stoichiometric amount, fluoride concentration in semiconductor fabrication can be reduced up to 10–20 mg/l. Additional processing is generally required to achieve the discharge concentration. Initial trial calcium precipitation experiments with the initial concentration of 217 mg/l could reduce concentration of F^- to 25 mg/l, the discharge limit in a single step process operation. Hence, the batch EC experiments were conducted with initial 25 mg/l F^- concentration.

2.1. Chemicals

In order to simulate the photovoltaic wastewater after calcium precipitation solutions of F^- in distilled water of 25 mg/l were prepared by dissolving NaF procured from Prolabo, Paris, France.

2.2. Electrocoagulation experiment

The electrocoagulation unit (Fig. 1) consists of 1 l electrochemical reactor with two iron electrodes connected in parallel. The electrodes dimensions are 100 × 85 mm. The distance between electrodes is 1 cm. The current density was maintained constant by means of a precision DC power supply (P.Fontaine MC 3030C). The fluorinated water is injected into the electrochemical reactor cell by means of the centrifugal Fontaine M7 feed pump, which allows flow rates of up to 460 L h and maintain well mixing of the CMP wastewater during the electrocoagulation process. The purity of the iron electrodes used was about 99.5%. Electrodes were sanded and washed with dilute HCl before each experiment. Experiments were conducted at a temperature around 25°C.

The defluoridation in small electrochemical reactor was performed with wastewater taken from UDTS – Algiers. The quality of parameters of wastewater are shown in Table 1. CaF_2 was presumed to be the only source of suspended solids after precipitation. The initial pH of the wastewater was 2.18 because a large quantity of hydrofluoric acid (HF) was used to etch wafers. Measured

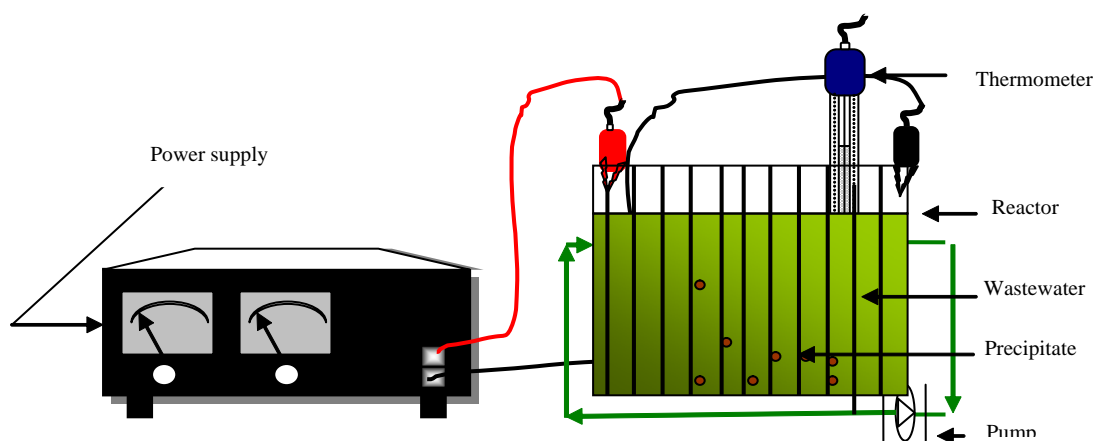


Fig. 1. Electrochemical reactor.

Table 1
Characteristics of photovoltaic wastewater

[F ⁻], mg/l	217
pH	2.18
Conductivity, $\mu\text{s}/\text{cm}$	1960
DCO, $\text{mg O}_2 \cdot \text{dm}^{-1}$	776
Color	Green

amounts of $\text{Ca}(\text{OH})_2$ salts were added to the wastewater to precipitate the fluoride ions and adjust the pH. Samples were drawn periodically during the experimentations for water quality measurements. Volume of the treated wastewater was put in the sludge settling column. A sludge settling test run lasted up to 3 h.

2.3. Chemical analysis

The PXRD analysis of the electrocoagulation by-products was carried out with a Bruker AXS D4 Endeavor diffractometer operating with a Cu K_α radiation source filtered with a graphic monochromator ($\lambda = 1.5406 \text{ \AA}$).

A selective ion sensor electrode [PF4L from Tacsell (Lyon)] was used to determine the F^- concentration according to the standard methods given by American Public Health Association [25]. To prevent the interference from other ions (Al^{3+} , Fe^{3+} , Cu^{2+} , Ca^{2+} , etc.), TISAB II buffer solution containing CDTA (cyclohexylenediaminetetraacetic acid, Orion Research, Inc.) was added to samples.

Philips spectrometer Magix with Rh tube and 4 kW power and Environmental MEB Philips (type ESEM XL30 FEG) combined with EDAX are used to characterize sludge. MEB pictures were taken at 10 kV at various magnifications.

FT-IR analysis were carried out by Perkin Elmer paragon 1000 spectrum RX and OMNIC software using potassium bromide pellets (sample : $\text{KBr} = 1 : 50$). The spectra were recorded in the range of $4000\text{--}400 \text{ cm}^{-1}$ with 2 cm^{-1} resolution.

3. Results and discussion

3.1. Effect of current density and operating time

Current density directly affected coagulant dosage and bubble generation rate, as well as the mixing intensity and mass transfer near electrodes [29], so increasing current density would accelerate the liberation rate of Fe^{2+} and OH^- ions. Fig. 2 describes the effect of current density on EC at constant electrode surface area (170 cm^2). Each of these experiments was conducted with the same initial concentration of 25 mg/l of F^- . After 60 min of EC, 9, 12 and 17 mg/l of F^- from the liquid phase was found to be transferred to the sludge phase at current densities of 29.41, 44.11 and 58.82 A/m^2 , respectively. The

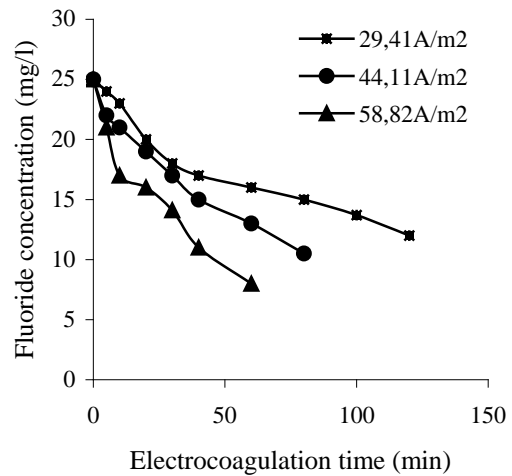


Fig. 2. Defluoridation of synthetic solution. $T = 20^\circ\text{C}$ and volume treated is 1 L.

maximum concentration limit as per Algerian discharge standard for F^- (15 mg/l) was obtained after 30 min of EC with 58.82 A/m^2 and 40 min 44.11 A/m^2 current density. The electrocoagulation process would take significantly longer to reach the discharge standard for fluoride for a current density of 29.41 A/m^2 . Therefore, effective removal of F^- from wastewater by electrocoagulation was observed at higher current densities.

Removal of fluoride by electrocoagulation previously presented was performed with wastewater obtained from UDTs, Algiers. Fluoride concentration of this wastewater after precipitation with lime is 25 mg/L . The effect of current density was studied at constant current density of 60 A/m^2 . According to Fig. 3, 40 min of operating time is sufficient for nearly reaching the discharge standard for

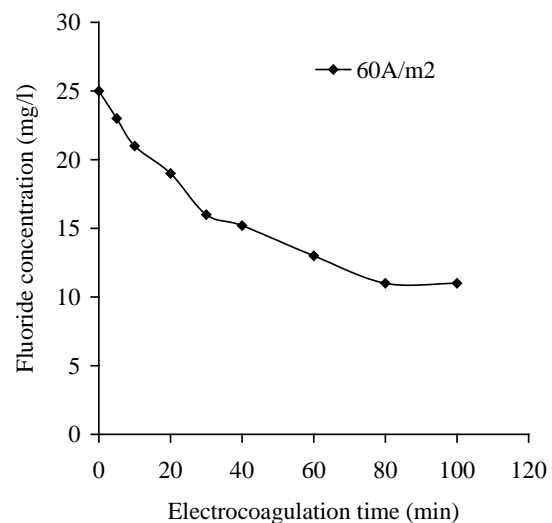


Fig. 3. Defluoridation of photovoltaic wastewater. $T = 20^\circ\text{C}$ and volume treated is 1 L.

fluoride removal. Removal of fluoride remains almost constant above 80 min. The discharge standards for fluoride were obtained in more time than using synthetic solution. This difference can be explained by the fact that co-existing anions are present in the fluoride containing wastewater. These co-existing anions are SO_4^{2-} , HCO_3^- and H_2PO_4^- . Competition of fluoride and these anions reduces the treatment efficiency of fluoride. This conclusion indicates that coexisting anions is a very important parameter as it affects the removal of fluoride in the EC process.

3.2. Sludge characteristics

3.2.1. FT-IR studies

The precipitate formed during electrocoagulation was further analyzed by FT-IR spectroscopic technique to understand the nature of adsorption of organic elements in the wastewater and its degradation products on iron oxy-hydroxide. The FT-IR spectrum of precipitate (Fig. 4a) shows a broad and intense band between $1440\text{--}1395\text{ cm}^{-1}$ and $1222\text{--}865\text{ cm}^{-1}$. This could be attributed to stretching vibrations of OH groups present in KOH, CH_3COOH and NH_4OH which are used in CMP of photovoltaic wastewater.

It is interesting to note that the associated bands in the region of $3700\text{--}3230\text{ cm}^{-1}$ ascribed to surface hydroxyls are absent (Fig. 4b). The strong and broad band at 1638 cm^{-1} (Fig. 4b) is generally attributed to N–H stretching vibrations. This band could indicate the presence of NH_4OH which is also used in CMP treatment of waters. The bands at 1754 cm^{-1} (Fig. 4c) could be assigned to C=O stretching vibrations of the acetic acid present in the analyzed solid sample.

3.2.2. X-ray diffraction

Diffractograms were obtained with a Bruker AXS D4 Endeavor diffractometer operating with a $\text{Cu K}\alpha$ radiation source filtered with a graphite monochromator ($\lambda = 1.5406\text{ \AA}$). The samples were wet ground to a fine powder (isopropyl alcohol from Sigma–Aldrich) and pressed into a sample holder. The XRD scans were recorded from 18° to $58^\circ 2\theta$. The spectrum scanning rate was set at $2\theta/\text{min}$. Experiments were run at 40 kV and 40 mA power. Fig. 5 shows a diffractogram of the precipitate products after EC. XRD diffractogram is very representative of lime (CaO). So we concluded that the substance presented by this XRD is lime, and it is due to the pH adjustment.

3.2.3. SEM/EDAX

To evaluate the structural features of the sludge that was generated by the electrocoagulation process, a series of scanning electron microscopy experiments were performed. The micrograph in Fig. 6 shows continuous spherical-shaped aggregates with diameters of around 100 nm. This information confirms that once the col-

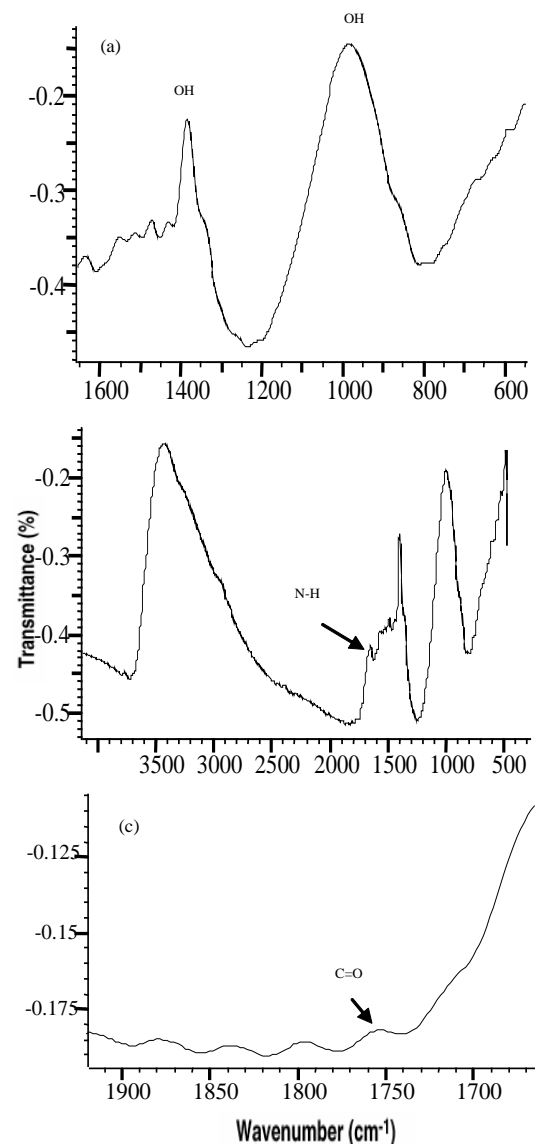


Fig. 4. FT-IR spectra of electrocoagulated sludge.

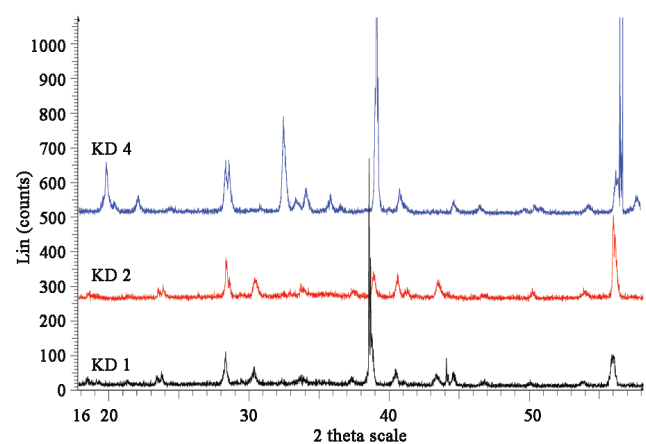


Fig. 5. XRD diffractogram of the sludge.

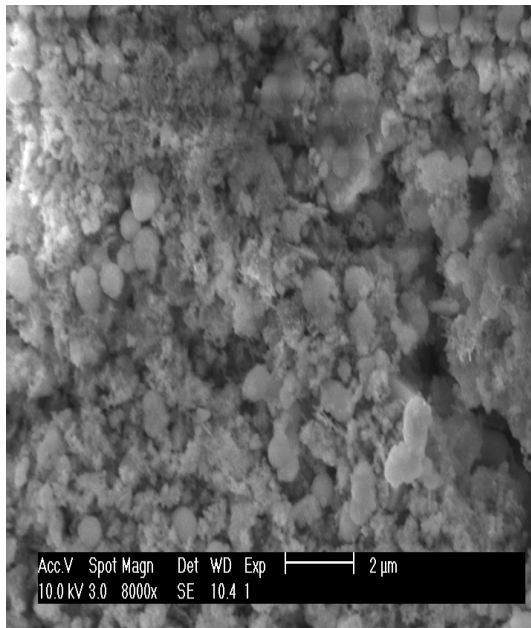


Fig. 6. MEB images of sludge in the wastewater.

loidal matter is destabilized, it can be separated from wastewater, and that iron generated by electrolysis forms complexes with the fluoride in the sludge. This technique also allows elemental analysis of the sludge by energy dispersive analysis of X-rays (EDAX) (image not presented here) in the electrocoagulation process. Table 2 shows the presence of the elements Fe, O, Na, Mg, Al, P, Cr, Mn and Ca. They confirm the presence of Fe released from anode (27.32 at.%), and oxygen generated from the anode material undergoes oxidation (57.97 at.%). Other elements detected in the sludge come from the precipitation with lime (calcium), chemicals used in the CMP treatment of waters and the scrap impurities of the Fe electrodes.

Table 2
EDAX ZAF Quantification (standardless)

Element	wt %	at %
O	31.66	57.97
Na	3.82	4.87
Mg	1.64	1.98
Al	0.33	0.36
P	0.83	0.78
Ca	7.83	5.72
Cr	1.14	0.64
Mn	0.67	0.36
Fe	52.08	27.32
Total	100.00	100.00

4. Conclusion

Electrocoagulation using bipolar iron electrodes of photovoltaic wastewater containing fluoride was investigated.

Synthetic solution of 1000 ml containing 25 mg/l F^- , having initial pH 6.4 after electrocoagulation at 58.82 A/m² current density for 30 min brings down the discharge standards to 15 mg/l.

Treatment of photovoltaic wastewater indicates that some cations and anions interfere with fluoride removal. Infrared analysis of the sludge confirmed the presence of organic compounds which can be attributed to the solvents used in CMP treatment. Finally, scanning electron microscopy and elemental analysis show the sludge morphology and the presence of Fe, O, Na, Mg, Al, P, Cr, Mn and Ca as its constituents. Additional studies are necessary to verify these results and further refine parameters for industrial application.

References

- [1] J. Zhu, H. Zhao and J. Ni, Fluoride distribution in electrocoagulation defluoridation process, *Separ. Purif. Technol.*, 56(2) (2007) 184–191.
- [2] World Health Organization: Fluoride in drinking water, WHO guidelines for drinking water quality, 2004, www.who.int/entity/water_sanitation_health/dwq/chemicals/fluoride.pdf.
- [3] H. Lounici, L. Addour, D. Belhocine, H. Grib, S. Nicolas, B. Bariou and N. Mameri, Study of a new technique for fluoride removal from water, *Desalination*, 114 (1997) 241–251.
- [4] S. Ghorai and K.K. Pant, Equilibrium, kinetics and breakthrough studies for adsorption of fluoride on activated alumina, *Separ. Purif. Technol.*, 42 (2005) 265–271.
- [5] G.L. He and S.R. Cao, Assessment of fluoride removal from drinking water by calcium phosphate systems, *Fluoride*, 29 (1996) 212–216.
- [6] M. Pinon-Miramontes, R.G. Bautista-Margulis and A. Perez-Hernandez, Removal of arsenic and fluoride from drinking water with cake alum and a polymeric anionic flocculent, *Fluoride*, 36 (2003) 122–128.
- [7] P.I. Ndiaye, P. Moulin, L. Dominguez, J.C. Millet and F. Charbit, Removal of fluoride from electronic industrial effluent by RO membrane separation, *Desalination*, 173 (2005) 25–32.
- [8] Z. Amor, B. Bariou, N. Mameri, M. Taky, S. Nicolas and A. Elmi-daoui, Fluoride removal from brackish water by electro dialysis, *Desalination*, 133 (2001) 215–223.
- [9] S.C. Li, Electro-chemical method to remove fluoride from drinking water, *Water Supply*, 3 (1985) 177–186.
- [10] N. Mameri, A.R. Yeddou, H. Lounici, D. Belhocine, H. Grib and B. Bariou, Defluoridation of septentrional Sahara water of north Africa by electrocoagulation process using bipolar aluminium electrodes, *Water Res.*, 32 (1998) 1604–1612.
- [11] M.M. Emamjomeh and M. Sivakumar, An empirical model for defluoridation by batch monopolar electrocoagulation/flotation (ECF) process, *J. Hazard. Mater.*, 131 (2006) 118–125.
- [12] N. Adhoum, L. Monser, N. Bellakhal and J. Belgaied, Treatment of electroplating wastewater containing Cu^{2+} , Zn^{2+} and $Cr(VI)$ by electrocoagulation, *J. Hazard. Mater.*, B 112 (2004) 207–213.
- [13] J. Ge, J. Qu, P. Lei and H. Liu, New bipolar electrocoagulation–electroflotation process for the treatment of laundry wastewater, *Separ. Purif. Technol.*, 36 (2004) 33–39.

- [14] E. Vorobiev, O. Larue, C. Vu and B. Durand, Electrocoagulation and coagulation by iron of latex particles in aqueous suspensions, *Separ. Purif. Technol.*, 31 (2003) 177–192.
- [15] M.N. Pons, A. Alinsafi, M. Khemis, J.P. Leclerc, A. Yaacoubi, A. Benhammou and A. Nejmeddine, Electro-coagulation of reactive textile dyes and textile wastewater, *Chem. Eng. Process.*, 44 (2005) 461–470.
- [16] Y.M. Slokar and A.M.L. Marechal, Methods of decoloration of textile wastewaters, *Dyes Pigments*, 37 (1998) 335–356.
- [17] M. Kobya, O.T. Can, M. Bayramoglu and M. Sozbir, Operating cost analysis of electrocoagulation of textile dye wastewater, *Separ. Purif. Technol.*, 37 (2004) 117–125.
- [18] M. Kobya, O.T. Can and M. Bayramoglu, Treatment of textile wastewaters by electrocoagulation using iron and aluminum electrodes, *J. Hazard. Mater.*, B 100 (2003) 163–178.
- [19] Y.A. Mohammad, R. Saurabh, K. Prashanth, V. Madhavi, S. Tejas, A.G. Jewel, K. Mehmet and L. David, Treatment of orange II azo-dye by electrocoagulation (EC) technique in a continuous flow cell using sacrificial iron electrodes, *J. Hazard. Mater.*, B 109 (2004) 165–171.
- [20] T. Kim, C. Park, E. Shin and S. Kim, Decolorization of disperse and reactive dyes by continuous electrocoagulation process, *Desalination*, 150 (2002) 165–175.
- [21] M. Kobya, O.T. Can and M. Bayramoglu, Decolorization of reactive dye solutions by electrocoagulation using aluminum electrodes, *Ind. Eng. Chem. Res.*, 42 (2003) 3391–3396.
- [22] N. Daneshvar, H. Ashassi-Sorkhabi and M.B. Kasiri, Decolorization of dye solution containing Acid Red 14 by electrocoagulation with a comparative investigation of different electrode connections, *J. Hazard. Mater.*, B 112 (2004) 55–62.
- [23] A.S. Koparal and Ü.B. Ögütveren, Removal of nitrate from aqueous solutions by electro-dialysis, *Int. J. Environ. Stud.*, 59(3) (2002) 323–329.
- [24] J.C. Donini, J. Kan, J. Szykarczuk, T.A. Hassan and K.L. Kar, The operating cost of electrocoagulation, *Can. J. Chem. Eng.*, 72 (1994) 1007–1012.
- [25] A.S. Koparal, The removal of salinity from produced formation by conventional and electrochemical methods, *Fresenius Environ. Bull.*, 11(12a) (2002) 1071–1077.
- [26] X. Chen, G.C. Chen and P.L. Yue, Separation of pollutants from restaurant wastewater by electrocoagulation, *Separ. Purif. Technol.*, 19 (2000) 65–76.
- [27] Ş. İrdemez, N. Demircioğlu, Y.Ş. Yıldız and Z. Bingül, The effects of current density and phosphate concentration on phosphate removal from wastewater by electrocoagulation using aluminum and iron plate electrodes, *Separ. Purif. Technol.*, 52 (2006) 218–223.
- [28] C.Y. Hu, S.L. Lo, W.H. Kuan and Y.D. Lee, Removal of fluoride from semiconductor wastewater by electrocoagulation–flotation, *Water Res.*, 39 (2005) 895–901.